Structural and biochemical characterization of human orphan DHRS10 reveals a novel cytosolic enzyme with steroid dehydrogenase activity

Petra Lukacik, Brigitte Keller, Gabor Bunkoczi, Kathryn L Kavanagh, Wen H Lee, Jerzy Adamski, Udo Oppermann

Structural and biochemical characterization of human orphan DHRS10 reveals a novel cytosolic enzyme with steroid dehydrogenase activity .

Petra Lukacik[†*], Brigitte Keller[‡], Gabor Bunkoczi[†], Kathryn Kavanagh[†], Wen Hwa Lee[†], Jerzy Adamski[‡], Udo Oppermann[†]

[†] Structural Genomics Consortium, University of Oxford, Oxford OX3 7LD, United Kingdom

[‡] GSF-National Research Center for Environment and Health, Institute for Experimental Genetics, Genome Analysis Center, Ingolstaedter Landstraße 1, 85764 Neuherberg, Germany

[*] Present address: Laboratory of Molecular Biology, NIDDK, National Institutes of Health, 50 South Drive, Room 4507, Bethesda, MD 20892-8030, U.S.A

Authors for correspondence: lukacikp@niddk.nih.gov, udo.oppermann@sgc.ox.ac.uk

Running title: Characterization of human DHRS10

SYNOPSIS

To this day, a significant proportion of the human genome remains devoid of functional characterisation. In this work we present evidence that the previously functionally un-characterised product of the human DHRS10 gene is endowed with 17β-hydroxysteroid dehydrogenase activity. 17β-hydroxysteroid dehydrogenase enzymes (17β-HSDs) are primarily involved in the metabolism of steroids at the C-17 position and also of other substrates such as fatty acids, prostaglandins and xenobiotics.

In vitro DHRS10 converts NAD^+ to NADH in the presence of estradiol, testosterone and 5-androstene-3β, 17β-diol. Furthermore, the product of estradiol oxidation, estrone, was identified in intact cells transfected with a construct plasmid encoding the DHRS10 protein. *In-situ* fluorescence hybridisation studies have revealed the cytoplasmic localisation of DHRS10. Along with tissue expression data this suggests a role for DHRS10 in the local inactivation of steroids in the CNS and placenta.

The crystal structure of the DHRS10 apoenzyme exhibits secondary structure of the short chain dehydrogenase/reductase (SDR) family: a Rossmann-fold with variable loops surrounding the active site. It also reveals a broad and deep active site cleft into which NAD^+ and estradiol can be docked in a catalytically competent orientation.

Key words:, steroid metabolism, 17β-hydroxysteroid dehydrogenase, pre-receptor control, short-chain dehydrogenase/reductase

Abbreviations: HSD: hydroxysteroid dehydrogenase; 17β-HSD: 17β-hydroxysteroid dehydrogenase; SDR: short-chain dehydrogenase/reductase; AKR: aldo-keto reductase; MDR: medium chain dehydrogenase/reductase;

INTRODUCTION

Hydroxysteroid dehydrogenases (HSDs) catalyze the oxidoreduction of hydroxyl/oxo groups of steroid hormones and in this manner regulate intracellular availability of steroid ligands to their nuclear receptors, and constitute a pre-receptor control mechanism [1, 2]. All mammalian hydroxysteroid dehydrogenases characterized to date are members of the aldo-keto reductases (AKR) [3], medium-chain dehydrogenases/reductases (MDR), or the short-chain dehydrogenase/reductase (SDR) families, with the clear majority of HSDs belonging to the latter family [4, 5]. The main steroid metabolizing activities regulating ligand access are oxidoreductases acting on positions 3, 11, 17 and 20, depending on the steroid hormone class. Whereas 3(α/β)-HSDs are involved in metabolism of all classes of steroid hormones, and 11β-HSDs and 20(α/β)-HSDs are restricted to glucocorticoids and progestins, 17β-HSDs play a central role in androgen and estrogen physiology. At present, 13 different isoforms of 17β-HSDs have been characterized and with the exception of 17β-HSD5 all are members of the SDR family [6-8]. They differ in nucleotide cofactor (NAD(H), NADP(H)) and steroid substrate (androgen/estrogen) specificity, subcellular compartmentalization and tissue-specific expression patterns. Accordingly, 17β-HSDs are numbered in chronological order according to their date of discovery. These HSDs can be grouped into *in vivo* oxidative enzymes (17β-HSD type 2, 4, 6, 8, 9, 10, 11, 12) catalyzing the NAD^+ dependent inactivation of steroid receptor ligands, or into *in vivo* reductive enzymes (17β-HSD type 1, 3, 5, 7) which are NADPH dependent and whose reactions lead to steroid receptor ligands. A specific feature of most 17β-HSDs is their remarkably broad substrate specificity, as observed in particular with fatty acyl-CoA derivatives (with type 4 and 10 17β-HSDs) or retinoic acid metabolites (observed with murine type 6 and 9 17β-HSDs). A multiple sequence alignment of human 17β-HSDs is given in Figure 1.

This work concerns the characterisation of the product of the human DHRS10 gene. We show that DHRS10 possesses 17β-HSD functionality both *in vivo* and *in vitro* and that its structure shares a common architecture with the majority of 17β-HSD enzymes. The *DHRS10* cDNA was previously isolated from retina epithelium [9], was initially termed retSDR3 and is currently annotated as “DHRS10” in the HUGO Gene Nomenclature

Database [10]. The encoded SDR enzyme was originally suspected to function in retinol metabolism as oxidoreductase, a role which could not be verified experimentally [9].

EXPERIMENTAL

Cloning of human DHRS10: A cDNA coding for human DHRS10 was obtained by gene synthesis using codon optimization for expression in *E. coli* (Genscript, NJ). The insert DNA was subcloned into a bacterial pET based expression vector, in frame into NdeI and BamHI sites, resulting in a variant containing an N-terminal His_6-tag, followed by a TEV protease cleavage site. For expression in cell culture or for Northern Blot analysis human DHRS10 cDNA was amplified from Hek293T cDNA using PCR with specific primers (for Northern Blot probe forward: 5′-GAG GTG AAA GAG GCC CAG AGT AG-3′, reverse: 5′-GTG ACC CGG CAC CTT GCT AAC-3′; for cloning into pcDNA3 (Invitrogen): 5′-TAT AGG ATC CAT GGC TAC GGG AAC GCG CTA TGC C-3′, reverse: 5′-TTA AGA ATT CTC AGG AAG GGA TAT CGG GGG CGT C-3′; for cloning into pcDNA4 myc-his (Invitrogen) 5′-TAT AGG ATC CGC CAC CAT GGC TAC GGG AAC GCG CTA TGC C-3′, reverse: 5′-TTA ACC GCG GGG AAG GGA TAT CGG GGG CGT CCA C-3′; for cloning into pEGFP-C2 (BD Biosciences, Heidelberg, Germany): 5′-TAT AGA ATT CAT GGC TAC GGG AAC GCG CTA TGC C-3′, reverse: 5′-TTA AGG ATC CTT CAG GAA GGG ATA TCG GGG GCG TC-3′). Inserts were verified by dideoxy sequence analysis using vector specific primers. For transfection, DNA was isolated using the PureYield Midi Kit (Promega, Mannheim, Germany) according to the manufacturer's instructions.

Heterologous expression in E. coli and purification of recombinant protein: The plasmid was transformed into Rosetta 2 (DE3) strain, and cells were grown overnight in 1 l Teriffic Broth containing 34 µg/ml chloramphenicol and 100 µg/ml ampicillin in a 2.5 l baffled flask at 37°C. Protein expression was induced by addition of 100 µM isopropylthiogalactoside (IPTG) at an OD of 0.6. The temperature was lowered to 15°C and the culture was continued for a further 20 h. The cells were harvested and stored at -80°C. The frozen cell pellet was resuspended in 30 ml of 50 mM Hepes pH 7.5, 500 mM NaCl, 5 mM imidazole and 0.5 mM Tris(2-carboxyethyl)phosphine (TCEP). The cells

were then disrupted using a high pressure homogenizer (Emulsiflex-C5, Avestin). Following centrifugation (17000 rpm, 4°C, 40 min) the clarified supernatant was passed through a 10 ml DE-52 column to remove DNA. The flow through was applied to a 2 ml Ni-NTA (Qiagen) column, washed with 20 ml of 50 mM Tris-HCl pH 7.5, 500 mM NaCl, 5 mM imidazole and 0.5 mM TCEP and eluted by raising the imidazole concentration to 250 mM. The eluted peak was loaded onto a S75 16/60 prep grade (GE/Amersham) gel filtration column in 10 mM HEPES, pH 7.5 500 mM NaCl, 5% glycerol and 0.5 mM TCEP. The essentially pure DHRS10 containing peak was concentrated (Vivaspin 20, Vivascience, MWCO 15K) to a final concentration of 12 mg/ml. After flash freezing in liquid nitrogen the protein was stored at -80°C for further analysis by crystallization or substrate screening. The mass of the purified product was verified by LC/MS on an Agilent LC/MSD TOF system (Agilent, UK).

Crystallization and structure determination: Crystals were grown by the sitting drop vapour diffusion method in 24 well sitting drop Cryschem plates (Hampton Research) at 20°C. 2 µl of the concentrated protein were mixed with 2 µl of 0.2 M magnesium acetate, 0.1 M sodium cacodylate, pH 6.5 and 20% (v/v) 2-methyl-2,4-pentanediol (MPD). The crystals were flash cooled in liquid nitrogen and X-ray diffraction data were collected at 100 K, at beamline 17-ID, Advanced Photon Source (APS), Argonne, Illinois, USA at a wavelength of 0.9794 Å. Data were indexed, integrated and scaled using the HKL2000 suite [11]. Phases were obtained by molecular replacement using the program PHASER [12]. Since a single highest homology model did not give a molecular replacement solution, a superimposed ensemble of eleven homologous structures (sequence identity between 30-38%) was used as a molecular replacement model. Refinement was initiated using strict NCS constraints in CNS [13]. However, in later stages it became apparent that the four tetramers in the asymmetric unit have A2B2 symmetry, the main difference between molecule A and B being the conformation of a 20-residue loop (residues 190-210). At this point refinement was continued with refmac5 [14], imposing tight NCS-restraints on appropriate molecules. Refinement was alternated with RESOLVE [15] run in prime-and-switch mode to remove model bias. Refinement converged to a

crystallographic R-factor of 0.181 and R_{free} of 0.229. The coordinates and structure factors were deposited at the protein data bank (PDB) with the code 1YDE.

Ligand docking: Two consecutive ligand docking procedures were performed according to the methodology described by Totrov and Abagyan [16, 17] and implemented in the program ICM v.3.4-1: one to position the NAD molecule into the cofactor binding pocket and a second one to dock the estradiol molecule into the active site of DHRS10. In both cases, grid maps representing different properties of the enzyme were computed. During the docking, either one of the torsional angles of the ligand was randomly changed or a pseudo-brownian move was performed. Each random change was followed by 100 steps of local conjugate-gradient minimization. The new conformation was accepted or rejected according to metropolis criteria using a temperature of 600 K. The length (number of Monte Carlo steps) of the docking run as well as the length of local minimization was determined automatically by an adaptive algorithm, depending on the size and number of flexible torsions in the ligand. The lowest energy conformation satisfying the absence of clashes after docking NAD^+ was incorporated into the structure file of DHRS10 and this was in turn used as receptor for the docking of estradiol. In this second docking, a positional restraint was imposed on the O17 atom of estradiol and the Tyr 154-OH, based on the catalytic mechanism of SDR enzymes [18, 19].

Substrate screening and kinetic analysis of purified recombinant human DHRS10: A compound library comprising 50 different steroids (androgen, estrogen, progestin, glucocorticoid hormones, bile acids and oxysterols; obtained from Sigma and Steraloids) with hydroxy/keto functions at position 3, 7, 11, 17, 20 and 21 were screened against purified human DHRS10 using a fluorescence-based assay on cofactor fluorescence change in a Spectramax M2 microplate reader (Molecular Devices). Steroids were dissolved in DMSO with stock solutions ranging from 5-20 mM, and were further diluted 1: 1000 in the assay mixture (oxidation: 50 mM Tris-HCl pH 8.5, 100 mM NaCl, 200 μM NAD^+ or $NADP^+$, 50 - 100 μg/ml enzyme, reduction: 50 mM Tris-HCl pH 7.5, 100 mM NaCl, 10 μM NADH or NADPH). Excitation was set to 340 nm, emission was at 460 nm, and the assay was conducted in 96 well plates (Costar). Initial hits from this

screen were verified by analysis of product formation using radioactively labeled steroids with an HPLC system coupled to online radioactivity detection. Kinetic analysis was carried out in 96 well plates as described above, or in single, 10 mm pathlength quartz cuvettes, by varying steroid substrate (200 nM – 100 µM) and cofactor (0.1 µM – 10 mM) concentrations. Initial velocities were converted into product formation using freshly prepared nucleotide cofactor solutions as standards, and data obtained were fitted by non-linear regression to the Michaelis-Menten equation using SigmaPlot or GraphPad software packages.

Cell culture and transfection: Hek293T, SaOS-2 and HeLa cells were grown under humidified standard conditions (37°C, 5% CO_2) in High Glucose Dulbecco's Modified Eagle Medium (Invitrogen, Karlsruhe, Germany) supplemented with 10% FBS (Biochrom AG, Berlin, Germany), 2 mM L-Glutamax I (Invitrogen), 100 U/ml penicillin/100µg/ml streptomycin. For transfection, FuGENE6 transfection reagent (Roche Biosciences, Mannheim, Germany) was used according to the manufacturer's instructions. For metabolite analysis, Hek293T cells were seeded onto 12-well plates (Nunc, Wiesbaden, Germany) and grown overnight before transfection. 24 h after transfection, 1 µl of [2,4,6,7-^{3}H(N)]-estradiol (final concentration 20 nM) (PerkinElmer, Wellesley, MA, USA) was added to cell culture medium and incubation was continued. Cell culture medium was collected at different time points, and purified with Strata-C18E columns (Phenomenex, Aschaffenburg, Germany). Samples were then analyzed on HPLC (Beckman, Fullerton, CA, USA) with 43% acetonitrile (in water) on a Luna C-18 column (Phenomenex). Conversion rates were obtained after integration of chromatograms and evaluated with 24Karat-software (Beckman). For analysis of subcellular localization, HeLa or SaOS-2 cells were seeded onto cover slides. After 24 h cells were transfected and grown for further 24 h. For counterstaining of mitochondria, MitoTracker Orange was used, for nuclear counterstaining Hoechst 33342 and for F-actin counterstaining, Alexa Fluor 568 phalloidin (all Invitrogen). For immunochemical detection of the myc-Tag 9B11 mouse mAb (Cell Signaling, NEB, Frankfurt a.M., Germany) was used as primary antibody, secondary antibody was Alexa Fluor 488 goat anti-mouse IgG (Invitrogen). After fixation and staining, cover slides were mounted onto

slides using Vectashield (Vector Laboratories, Burlingame, CA, USA). Subcellular localization was analyzed by Zeiss Axiophot fluorescence microscope (Carl Zeiss, Oberkochen, Germany) with the ISIS (MetaSystems, Altlussheim, Germany) image processing software.

Expression analysis of DHRS10 in human tissues: FirstChoice Northern Blot Human Blot II (Ambion) was used with recommended wash solutions and Ultrahyb hybridization solution according to manufacturer's instructions. The PCR-product used as probe used for Northern blot was labelled with Strip-EZ DNA Kit (Ambion, Huntington, UK). Radioactively labelled nucleotides were purchased from Amersham Biosciences (Uppsala, Sweden). Detection was done by autoradiography using BioMax XAR films (Kodak Industrie, Chalon-sur-Saône, Cedex, France).

RESULTS

Expression, purification and activity of human DHRS10: Full length DHRS10 was expressed and purified in a two step chromatographic procedure yielding about 20 mg per litre of culture. The purified protein was judged homogeneous by SDS-PAGE and mass spectrometry (data not shown), and was found suitable for subsequent use in substrate screening, kinetic and crystallographic studies. A fluorescent assay was used to carry out substrate screening against a collection of different steroids. Purified DHRS10 enzyme turned over NAD^+ to NADH in the presence of estradiol, testosterone or 5-androstene-3β, 17β-diol. Michaelis-Menten kinetics were observed for estradiol and 5-androstene-3β, 17β-diol; with K_m values of 5.6 ± 1.7 and 13.6 ± 1.6 μM, and V_{max} values of 2.5 ± 1.0 and 9.1 ± 1.6 nmol NADH $min^{-1}mg^{-1}$ for estradiol and 5-androstene-3β, 17β-diol respectively. However non saturable kinetics were found for testosterone (Figure 2, Table 2). No conversion was observed in the presence of NADP(H) or with β-OH-butyryl CoA which is a *bona fide* substrate for other 17β-HSDs such as 17β-HSD4 and 17β-HSD10 (Table 2).

DHRS10 activity in intact cells: In order to verify steroid conversion by DHRS10 in intact cells and to investigate the direction of the DHRS10 reaction *in vivo*, Hek293T

cells were transfected with an expression plasmid encoding DHRS10 and exposed to 20 nM radiolabeled estradiol. The transfected cells efficiently oxidised estradiol to estrone as revealed by HPLC analysis of the supernatant (Figure 2). This conversion rate is significantly faster in comparison to that of mock transfected cells (pcDNA3 vector only). Therefore, intact cells expressing DHRS10 can indeed oxidize steroids at physiological hormone concentrations.

Crystal Structure of DHRS10: Following extensive crystallisation trials the purified protein yielded well diffracting crystals suitable for crystallographic analysis. The crystal structure of DHRS10 was solved by molecular replacement to a resolution of 2.4 Å, and a summary of data processing and refinement statistics is compiled in Table 1. The asymmetric unit contains sixteen DHRS10 monomers arranged as four tetramers with 222-point group symmetry. Each monomer comprises two distinct regions (Figure 3): The first region is a Rossmann-fold built up of a central β-sheet core consisting of 7 parallel β-strands (βA-βG) sandwiched between two arrays of parallel helices (αB-αG). This region has a characteristic nucleotide cofactor (NAD(H) or NADP(H)) binding motif T-G-X3-G-X-G located near its N-terminus. Residue Asp 40 is present at the C-terminal end of the second β-strand (βB). In SDR structures the presence of an acidic residue at this location indicates a NAD(H) versus NAD(P) selectivity, since the carboxylate group is in a favourable location to interact with the 2′ and 3′ OH groups of the adenosine ribose of NAD. Accordingly, this residue prohibits NADP(H) binding by repelling the negative charge on the 2′ phosphate and thus confers NAD(H) specificity to DHRS10 [20]. Kinetic analysis (cf above) confirmed NAD(H) as the cofactor for the DHRS10 reaction. Also within this region is a very short α-helix (αEF) inserted between αE and βF and encompassing residues 142-147. A second region contains two additional alpha-helical elements αFG1 (residues 189-197) and αFG2 (residues 201-212) that are inserted between βF and αG. As with all SDRs whose structures have been determined so far, this second region is more variable and is responsible for substrate binding.

In the apostructure determined, a broad active site cleft lies between the two regions (Figures 3 and 5). Apart from the highly conserved catalytic triad that consists of Ser 141,

Tyr 154 and Lys 158, this active site cleft contains a number of hydrophobic residues potentially involved in binding of hydrophobic substrates (Figure 4).

Ligand docking into the DHRS10 active site: Although numerous co-crystallisation experiments were attempted, DHRS10 crystallised as an apoenzyme with no cofactor or substrate in the active site. In order to understand the interactions of DHRS10 with its cofactor and substrate on a molecular level, *in silico* ligand docking was performed on the protein monomer.

Starting models for the estradiol substrate and NAD^+ cofactor were obtained fom the crystal structure of rat 17β-HSD10 (also known as type II 3-hydroxyacyl-CoA dehydrogenase, PDB code 1E6W). The *in silico* docking of NAD^+ yielded a very satisfactory conformation for both protein and cofactor. The docked NAD^+ molecule presented a rmsd of 0.855 Å for all atoms when compared to the NAD^+ cofactor of type II 3-hydroxyacyl-CoA dehydrogenase. The small difference was expected since the cofactor binding pocket is not completely conserved and small variations in the binding pose are expected in these situations. In spite of this, the overall geometry of the DHRS10 binding pocket has been preserved and NAD^+ could be docked in a manner very similar to that observed in 1E6W.

The docking of estradiol to the DHRS10-NAD^+ model can be achieved by placing the atom O17 of estradiol within the proximity of the catalytic tyrosine (Tyr 154) while keeping the atom C17 close enough to C4 of the nicotinamide for hydride transfer during catalysis (3.4 Å) (Figure 4). Consequently the C17 hydroxyl is within hydrogen bonding distance of Tyr 154 (3.2 Å) and Ser 141 (3.0 Å). In this conformation the remainder of the environment of the estradiol molecule is made up of mixture of polar and non-polar residues: His 93, Val 143, Gln 148, Trp 192 and Asn 186 lie within 4 Å of the estradiol molecule and contribute to van der Waals interactions with estradiol. There are no residues that contribute to additional hydrogen bonding with estradiol.

A structural comparison of DHRS10 with docked NAD/estradiol was carried out to the crystal structure of the ternary complex of 17β-HSD1 with NADP/estradiol (PDB code 1FDT), apo 17β-HSD1 (PDB code 1BHS) and to other structures of members of the 17β-HSD family. The DHRS10 molecule possesses a prominent broad and open active site

cleft that is not observed in 17β-HSD1 (Figure 5) or other 17β-HSDs (data not shown). Within this cleft the docked estradiol molecule sits rather loosely. Again this is in contrast to 17β-HSD1 where estradiol interactions are better defined. Here the estradiol is stabilized by three rather than two hydrogen bonds: two to the catalytic serine and tyrosine and an additional hydrogen bond between estradiol O3 and Nε2 of His 221 [21]. Additionally, a number of neighbouring residues contributes to hydrophobic interactions with the core of the steroid.

Nonetheless the docking procedure employed within does not take into account the possible conformational changes to the DHRS10 structure induced by binding of cofactor or substrate. Consequently the milieu of the estradiol could be significantly different in the secondary or tertiary complex of DHRS10.

Interestingly a comparison of the apo and ternary complex structure of 17β-HSD1 reveals that although some structural rearrangement does occur in the loop connecting βF and αFG1, overall the active site remains closed in both structures (Figure 5).

Subcellular Localisation of DHRS10: Immuno-fluorescence subcellular localisation studies were carried out where a DHRS10 construct with a myc-tag at its N-terminus was probed with a primary anti-myc monoclonal mouse antibody and a secondary fluorescent antibody. To eliminate the possibility of the N-terminal tag interfering with the proper targeting of the DHRS10 protein, *in situ* fluorescence experiments were also carried out on HeLa cells expressing human DHRS10 with a GFP tag at its C-terminus. In both cases the studies clearly reveal the cytoplasmic localisation of DHRS10 protein (Figure 6). No mitochondrial or nuclear targeting could be observed using fluorescent mitochondrial (data not shown) and nuclear reporter dyes.

Expression analysis of DHRS10 in human tissues: Northern blot analysis using a radioactively labeled probe of DHRS10 was carried out on selected human tissues (Figure 7). High expression is observed in brain, liver and placenta, whereas no or low signals are observed in small intestine, colon, pancreas, spleen, and gonads (testes and ovary). Two distinct sizes of specific signals are observed (approximately 5.5 and 7 kbp),

indicating two distinct transcription or splicing sites in brain and placenta, whereas in liver only one mRNA species is observed (Figure 7).

DISCUSSION

In this study we have identified DHRS10 as a cytosolic SDR enzyme with 17β-HSD activity on steroid substrates. Out of the human tissues investigated the highest levels of DHRS10 expression were observed in the brain, liver and placenta.

The DHRS10 gene was initially cloned in an attempt to define retinoid metabolizing enzymes, however, this function was excluded after heterologous expression [9]. To our knowledge, no further functional studies are available on this human gene or any mammalian ortholog. To investigate the structural and functional features of the enzyme, we determined the crystal structure and correlate these results to functional analyses. To this end, experimental structure determination appears to be essential to derive at functional conclusions. We performed homology modelling of human DHRS10 using the two closest available structures as templates, namely Rv2002 gene product from *Mycobacterium tuberculosis* (PDB code 1NFQ) and TT0321 from *Thermus thermophilus* HB8 (PDB code 2D1Y), both with 38% sequence identity. Although the predicted folding was very similar to the experimental structure, and homology modeling could be performed in a satisfactory manner for most of the molecule, an important active site segment comprising ~14 residues was not correctly predicted due to high sequence variation. Thus, a docking analysis to suggest possible substrates for de-orphanisation of DHRS10 could not be carried out due to the lack of reliable templates for this critical portion of the structure. Structure prediction for a segment with such size to the level required for de-orphanisation via docking methods is therefore still beyond the reach of present technology.

In common with the majority of 17β-HSDs the crystal structure displays the typical characteristics of the short-chain dehydrogenase/reductase family with a largely conserved fold and the presence of catalytically important residues Asn 114, Ser 141, Tyr 154, Lys 158 (fig 1) [19]. Interestingly, a deep and broad active site cleft is found within the DHRS10 structure. This feature is more prominent than in other 17β-HSDs for which

three dimensional structures have been determined to date. As well as demonstrating that this protein converts 17β-OH steroids such as estradiol to estrone both *in vivo* and *in vitro,* we also show that NAD^+ and estradiol can be docked within the cleft in a catalytically competent conformation. This study reveals the molecular details of the enzyme/substrate/cofactor interaction and shows that the estradiol substrate sits rather loosely within the active site cleft. Such a conformation has several possible implications. Firstly, it might explain the rather low catalytic turnover value for the *in vitro* DHRS10 reaction. However, the low k_{cat} value for DHRS10 is not entirely unusual and a number of other SDR enzymes have similarly low k_{cat} values for substrates that have nevertheless been shown to be relevant in their physiological context. The latter is exemplified by human 11β-HSD1 which carries out metabolic activation of the glucocorticoid hormone cortisol from the precursor cortisone. The determined k_{cat} for cortisone reduction is only about 20 times higher [22] than the k_{cat} value for the DHRS10/NAD^+/estradiol reaction, yet the *in vivo* importance of this reaction has been demonstrated on a number of occasions and is highlighted by its involvement in metabolic disease such as obesity and insulin resistance [23-26]. Furthermore, human 17β-HSD10 displays an about 10 fold higher k_{cat} than DHRS10/NAD^+/estradiol [22], however the K_m of 17β-HSD10 for this reaction is about 5-fold higher, suggesting that 17β-HSD10 and DHRS10 have similar k_{cat}/K_m values. Secondly, the broad active site cleft suggests that the DHRS10 enzyme might have other substrate specificities besides estradiol since the active site cleft is wide enough to accommodate larger substrates than steroid molecules. This broad substrate spectrum appears to be a hallmark for 17β-HSDs, and accordingly, broad substrate specificity has been demonstrated for a number of 17β-HSDs such as type 4, 6 and 10 [2, 8]. In addition, wider substrate specificity of DHRS10 is also possible, as deduced from a phylogenetic analysis that shows that DHRS10 clusters with SDR proteins such as peroxisomal trans-2-enoyl-CoA reductase (PECR) [27, 28] and mitochondrial 2,4-dienoyl CoA reductase 1 (DECR1) [29, 30] whose primary roles are in converting fatty-acyl CoAs rather than steroids (data not shown). However, an initial screen with a limited number of compounds (comprising > 200 compounds including CoA derivatives) as possible substrates or ligands for SDR enzymes did not reveal any significant binding except for estrogen-based steroids (data not shown). Thirdly, it is also possible that the

extensive and open active site cleft is a feature of the apoenzyme and that the cleft might undergo a conformational change and close when ligands are bound.

Together with the expression observed in tissues such as liver, brain and placenta, the proven *in vivo* and *in vitro* function of DHRS10 as oxidative 17β-hydroxy dehydrogenase, suggest possible roles for DHRS10 in the local regulation of active steroid hormones levels [1, 2]. DHRS10 would therefore be responsible for steroid inactivation similar to 17β-HSD2. However, as shown in this work the tissue distribution of DHRS10 is distinct to that reported for type 2 [31, 32] and because of that a tissue-specific function is postulated. This is in analogy to other 17β- or 11β-HSD enzymes that constitute critical determinants of steroid hormone physiology [1]. It appears in several situations essential that steroid ligands are excluded from their receptors, as is the case with glucocorticoids and the mineralocorticoid receptor.

Our *in vitro* data indicate that DHRS10 is involved in the local inactivation of 5-androstene-3β, 17β-diol and of estradiol, and taken together with the initial expression data obtained in this study, suggest possible functional roles mainly in the placenta and the CNS. The activity and expression in the CNS thus adds DHRS10 isozyme to the complexity of estrogen and DHEA metabolizing steroid dehydrogenases observed in a study conducted by Steckelbroeck et al [33], noting multiple 17β-HSDs involved in human brain tissues. The weak estrogenic steroid 5-androstene-3β, 17β-diol is an important metabolic intermediate in the peripheral sex steroid synthesis starting from DHEA. 5-androstene-3β, 17β-diol is secreted by the adrenal gland, and like the sex steroids display important functions in the brain such as hippocampal neurogenesis and neural survival [34]. Estrogens have an extensive range of effects on the brain [35]. These include effects on brain development [36], centrally regulated effects on reproduction, mood [37], cognition [38], protection from neurotoxins/neurodegeneration or injury [39, 40], neuron plasticity [41], transcription of neuropeptides [42] and regulative effects on the enzymes that affect the synthesis and turnover of classical neurotransmitters e.g. serotonin [43] and dopamine [44] .

It is clear that the cytosolic localisation of DHRS10 could allow *control by access* by limiting exogenously and endogenously produced active estrogen (estradiol) from reaching to estrogen ERα/β receptors located in the nucleus. Interestingly surface

membrane associated estrogen receptors, whose existence have also been recently demonstrated [45, 46], would allow bypass of such control.

Taken together, we have provided a structural and functional characterization of a yet poorly annotated mammalian gene product. Further studies concerning temporal and spatial expression patterns, animal studies, as well as a search for other possible substrate activities will be mandatory for the additional annotation of this SDR member.

ACKNOWLEDGEMENTS

The Structural Genomics Consortium is a registered charity (number 1097737) funded by the Wellcome Trust, GlaxoSmithKline, Genome Canada, the Canadian Institutes of Health Research, the Ontario Innovation Trust, the Ontario Research and Development Challenge Fund, the Canadian Foundation for Innovation; Vinnova, Knut and Alice Wallenberg foundation; and Karolinska Institutet. Data collection by F. von Delft is gratefully acknowledged.

REFERENCES

1 Nobel, S., Abrahmsen, L. and Oppermann, U. (2001) Metabolic conversion as a pre-receptor control mechanism for lipophilic hormones. Eur. J. Biochem. **268**, 4113-4125

2 Mindnich, R., Moller, G. and Adamski, J. (2004) The role of 17 beta-hydroxysteroid dehydrogenases. Mol. Cell. Endocrinol. **218**, 7-20

3 Jez, J. M. and Penning, T. M. (2001) The aldo-keto reductase (AKR) superfamily: an update. Chem. Biol. Interact. **130-132**, 499-525

4 Marschall, H. U., Oppermann, U. C., Svensson, S., Nordling, E., Persson, B., Hoog, J. O. and Jornvall, H. (2000) Human liver class I alcohol dehydrogenase gammagamma isozyme: the sole cytosolic 3beta-hydroxysteroid dehydrogenase of iso bile acids. Hepatology **31**, 990-996

5 Oppermann, U. C., Filling, C. and Jornvall, H. (2001) Forms and functions of human SDR enzymes. Chem. Biol. Interact. **130-132**, 699-705

6 Adamski, J. and Jakob, F. J. (2001) A guide to 17beta-hydroxysteroid dehydrogenases. Mol. Cell. Endocrinol. **171**, 1-4

7 Penning, T. M., Burczynski, M. E., Jez, J. M., Lin, H. K., Ma, H., Moore, M., Ratnam, K. and Palackal, N. (2001) Structure-function aspects and inhibitor design of type 5 17beta-hydroxysteroid dehydrogenase (AKR1C3). Mol. Cell. Endocrinol. **171**, 137-149

8 Lukacik, P., Kavanagh, K. L. and Oppermann, U. (2006) Structure and function of human 17beta-hydroxysteroid dehydrogenases. Mol. Cell. Endocrinol. **248**, 61-71

9 Haeseleer, F. and Palczewski, K. (2000) Short-chain dehydrogenases/reductases in retina. Methods Enzymol. **316**, 372-383

10 Wain, H. M., Lush, M. J., Ducluzeau, F., Khodiyar, V. K. and Povey, S. (2004) Genew: the Human Gene Nomenclature Database, 2004 updates. Nucleic Acids Res. **32**, D255-257

11 Otwinowski, Z., W. Minor (1997) Processing of X-ray Diffraction Data Collected in Oscillation Mode. Academic Press (New York)

12 Storoni, L. C., McCoy, A. J. and Read, R. J. (2004) Likelihood-enhanced fast rotation functions. Acta Crystallographica Section D **60**, 432-438

13 Brunger, A. T., Adams, P. D., Clore, G. M., DeLano, W. L., Gros, P., Grosse-Kunstleve, R. W., Jiang, J.-S., Kuszewski, J., Nilges, M., Pannu, N. S., Read, R. J., Rice, L. M., Simonson, T. and Warren, G. L. (1998) Crystallography & NMR System: A New Software Suite for Macromolecular Structure Determination. Acta Crystallographica Section D **54**, 905-921

14 Murshudov, G. N., Vagin, A. A. and Dodson, E. J. (1997) Refinement of Macromolecular Structures by the Maximum-Likelihood Method. Acta Crystallographica Section D **53**, 240-255

15 Terwilliger, T. (2000) Maximum-likelihood density modification. Acta Crystallographica Section D **56**, 965-972

16 Abagyan, R. A. and Totrov, M. M. (1997) Contact area difference (CAD): a robust measure to evaluate accuracy of protein models. J. Mol. Biol. **268**, 678-685

17 Abagyan, R. and Totrov, M. (2001) High-throughput docking for lead generation. Curr. Opin. Chem. Biol. **5**, 375-382

18 Jornvall, H., Persson, B., Krook, M., Atrian, S., Gonzalez-Duarte, R., Jeffery, J. and Ghosh, D. (1995) Short-chain dehydrogenases/reductases (SDR). Biochemistry **34**, 6003-6013

19 Filling, C., Berndt, K. D., Benach, J., Knapp, S., Prozorovski, T., Nordling, E., Ladenstein, R., Jornvall, H. and Oppermann, U. (2002) Critical residues for structure and catalysis in short-chain dehydrogenases/reductases. J. Biol. Chem. **277**, 25677-25684

20 Kallberg, Y., Oppermann, U., Jornvall, H. and Persson, B. (2002) Short-chain dehydrogenases/reductases (SDRs). Eur. J. Biochem. **269**, 4409-4417

21 Breton, R., Housset, D., Mazza, C. and Fontecilla-Camps, J. C. (1996) The structure of a complex of human 17beta-hydroxysteroid dehydrogenase with estradiol and NADP+ identifies two principal targets for the design of inhibitors. Structure **4**, 905-915

22 Shafqat, N., Elleby, B., Svensson, S., Shafqat, J., Jornvall, H., Abrahmsen, L. and Oppermann, U. (2003) Comparative enzymology of 11 beta -hydroxysteroid dehydrogenase type 1 from glucocorticoid resistant (Guinea pig) versus sensitive (human) species. J. Biol. Chem. **278**, 2030-2035

23 Tomlinson, J. W., Moore, J. S., Clark, P. M., Holder, G., Shakespeare, L. and Stewart, P. M. (2004) Weight loss increases 11beta-hydroxysteroid dehydrogenase type 1 expression in human adipose tissue. J. Clin. Endocrinol. Metab. **89**, 2711-2716

24 Draper, N., Echwald, S. M., Lavery, G. G., Walker, E. A., Fraser, R., Davies, E., Sorensen, T. I., Astrup, A., Adamski, J., Hewison, M., Connell, J. M., Pedersen, O. and Stewart, P. M. (2002) Association studies between microsatellite markers within the gene encoding human 11beta-hydroxysteroid dehydrogenase type 1 and body mass index, waist to hip ratio, and glucocorticoid metabolism. J. Clin. Endocrinol. Metab. **87**, 4984-4990

25 Engeli, S., Bohnke, J., Feldpausch, M., Gorzelniak, K., Heintze, U., Janke, J., Luft, F. C. and Sharma, A. M. (2004) Regulation of 11beta-HSD genes in human adipose tissue: influence of central obesity and weight loss. Obes. Res. **12**, 9-17

26 Seckl, J. R., Morton, N. M., Chapman, K. E. and Walker, B. R. (2004) Glucocorticoids and 11beta-hydroxysteroid dehydrogenase in adipose tissue. Recent Prog. Horm. Res. **59**, 359-393

27 Amery, L., Mannaerts, G. P., Subramani, S., Van Veldhoven, P. P. and Fransen, M. (2001) Identification of a novel human peroxisomal 2,4-dienoyl-CoA reductase related protein using the M13 phage protein VI phage display technology. Comb. Chem. High Throughput Screen. **4**, 545-552

28 Das, A. K., Uhler, M. D. and Hajra, A. K. (2000) Molecular cloning and expression of mammalian peroxisomal trans-2-enoyl-coenzyme A reductase cDNAs. J. Biol. Chem. **275**, 24333-24340

29 Helander, H. M., Koivuranta, K. T., Horelli-Kuitunen, N., Palvimo, J. J., Palotie, A. and Hiltunen, J. K. (1997) Molecular cloning and characterization of the human mitochondrial 2,4-dienoyl-CoA reductase gene (DECR). Genomics **46**, 112-119

30 Koivuranta, K. T., Hakkola, E. H. and Hiltunen, J. K. (1994) Isolation and characterization of cDNA for human 120 kDa mitochondrial 2,4-dienoyl-coenzyme A reductase. Biochem. J. **304 (Pt 3)**, 787-792

31 Mustonen, M. V., Isomaa, V. V., Vaskivuo, T., Tapanainen, J., Poutanen, M. H., Stenback, F., Vihko, R. K. and Vihko, P. T. (1998) Human 17beta-hydroxysteroid dehydrogenase type 2 messenger ribonucleic acid expression and localization in term placenta and in endometrium during the menstrual cycle. J. Clin. Endocrinol. Metab. **83**, 1319-1324

32 Miettinen, M. M., Mustonen, M. V., Poutanen, M. H., Isomaa, V. V. and Vihko, R. K. (1996) Human 17 beta-hydroxysteroid dehydrogenase type 1 and type 2 isoenzymes have opposite activities in cultured cells and characteristic cell- and tissue-specific expression. Biochem. J. **314 (Pt 3)**, 839-845

33 Steckelbroeck, S., Watzka, M., Lutjohann, D., Makiola, P., Nassen, A., Hans, V. H., Clusmann, H., Reissinger, A., Ludwig, M., Siekmann, L. and Klingmuller, D. (2002) Characterization of the dehydroepiandrosterone (DHEA) metabolism via oxysterol 7alpha-hydroxylase and 17-ketosteroid reductase activity in the human brain. J. Neurochem. **83**, 713-726

34 Karishma, K. K. and Herbert, J. (2002) Dehydroepiandrosterone (DHEA) stimulates neurogenesis in the hippocampus of the rat, promotes survival of newly formed neurons and prevents corticosterone-induced suppression. Eur. J. Neurosci. **16**, 445-453

35 Wang, L., Andersson, S., Warner, M. and Gustafsson, J. A. (2002) Estrogen actions in the brain. Sci. STKE **2002**, PE29

36 Beyer, C. (1999) Estrogen and the developing mammalian brain. Anat. Embryol. (Berl). **199**, 379-390

37 Young, E. A. and Korszun, A. (2002) The hypothalamic-pituitary-gonadal axis in mood disorders. Endocrinol. Metab. Clin. North Am. **31**, 63-78

38 Pinkerton, J. V. and Henderson, V. W. (2005) Estrogen and cognition, with a focus on Alzheimer's disease. Semin. Reprod. Med. **23**, 172-179

39 Marin, R., Guerra, B., Alonso, R., Ramirez, C. M. and Diaz, M. (2005) Estrogen activates classical and alternative mechanisms to orchestrate neuroprotection. Curr. Neurovasc. Res. **2**, 287-301

40 Wise, P. M., Dubal, D. B., Rau, S. W., Brown, C. M. and Suzuki, S. (2005) Are estrogens protective or risk factors in brain injury and neurodegeneration? Reevaluation after the Women's health initiative. Endocr. Rev. **26**, 308-312

41 Cooke, B. M. and Woolley, C. S. (2005) Gonadal hormone modulation of dendrites in the mammalian CNS. J. Neurobiol. **64**, 34-46

42 Harlan, R. E. (1988) Regulation of neuropeptide gene expression by steroid hormones. Mol. Neurobiol. **2**, 183-200

43 Osterlund, M. K., Halldin, C. and Hurd, Y. L. (2000) Effects of chronic 17beta-estradiol treatment on the serotonin 5-HT(1A) receptor mRNA and binding levels in the rat brain. Synapse **35**, 39-44

44 Di Paolo, T. (1994) Modulation of brain dopamine transmission by sex steroids. Rev. Neurosci. **5**, 27-41

45 Toran-Allerand, C. D. (2004) Estrogen and the brain: beyond ER-alpha and ER-beta. Exp. Gerontol. **39**, 1579-1586

46 Toran-Allerand, C. D., Guan, X., MacLusky, N. J., Horvath, T. L., Diano, S., Singh, M., Connolly, E. S., Jr., Nethrapalli, I. S. and Tinnikov, A. A. (2002) ER-

X: a novel, plasma membrane-associated, putative estrogen receptor that is regulated during development and after ischemic brain injury. J. Neurosci. **22**, 8391-8401

Table 1: Data processing and refinement statistics.

	DHRS10 crystal
Data Processing	
Wavelength (Å)	0.9794
Space group	P1211
Unit cell parameters (Å,°)	167.1 98.8 167.5 90.0 115.9 90.0
Resolution range (outer shell)(Å)	82.6-2.4 (2.5-2.4)
Observed Reflections (outer shell)	558993(13185)
Unique reflections (outer shell)	176307(12096)
Completeness (outer shell)(%)	91.9(55.2)
Mean I/σI (outer shell)	9.1(1.6)
Multiplicity (outer shell)	2.9 (1.1)
R_{MERGE} (outer shell)	0.117(0.575)
V_M ($Å^3Da^{-1}$)	2.5
Refinement	
Protein atoms	29419
Protein residues (per chain)	A:250, B:247, C:250, D:255, E:250, F:256, G:247, H:254, I:247, J:255, K:250, L:255, M:244, N:240, O:247, P:254
Waters in model	1251
R_{WORK}	0.181
R_{FREE}	0.229
RMSD bond lengths (Å)	0.016
RMSD bond angles (°)	1.505
Average B factor ($Å^2$)	
Main Chain (per chain)	4.485
Side Chain (per chain)	7.187
Waters	4.650
PDB ID	1YDE

Biochemical Journal Immediate Publication. Published on 27 Oct 2006 as manuscript BJ20061319

Table 2: Kinetic parameters determined for human DHRS10 using NAD^+ as cofactor. Abbreviations: na: no activity detectable; *: estimated K_m and V_{max}, due to non saturable kinetics. Number of experiments: n=3-4.

Substrate	**K_m (µM)**	**V_{max} (nmol NADH $min^{-1}mg^{-1}$)**	**k_{cat} (min^{-1})**
estradiol	5.6 ± 1.7	2.5 ± 1.0	0.076 ± 0.026
testosterone*	470*	2.6*	-
5-androstene-3β, 17β-diol	13.6 ± 1.6	9.1 ± 1.6	0.28 ± 0.05
OH-butyryl-CoA	na	-	-
$NADP^+$	na	-	-

Biochemical Journal Immediate Publication. Published on 27 Oct 2006 as manuscript BJ20061319

Figure 1:

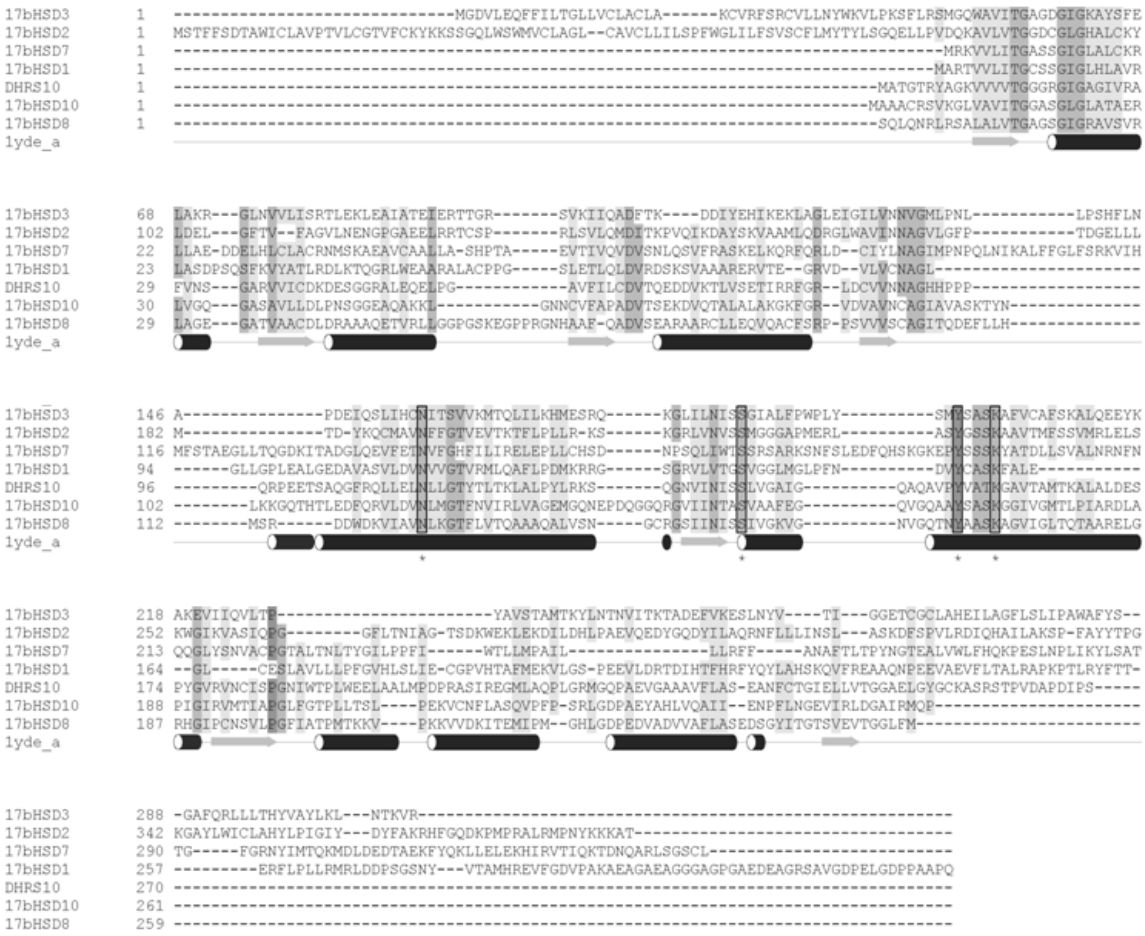

Biochemical Journal Immediate Publication. Published on 27 Oct 2006 as manuscript BJ20061319

Figure 2

a)

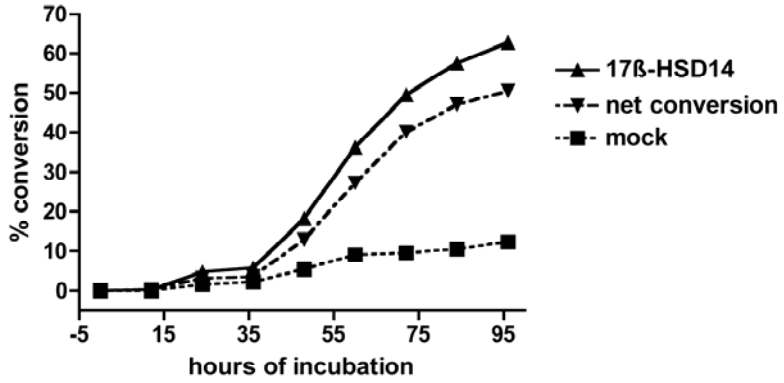

b)

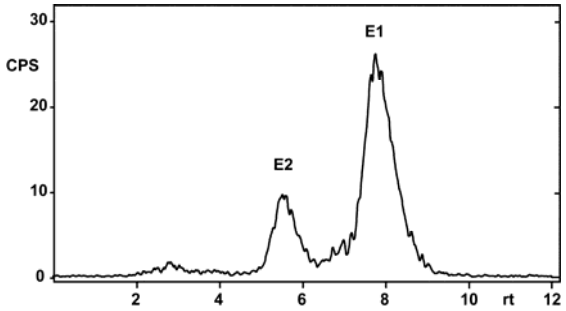

c)

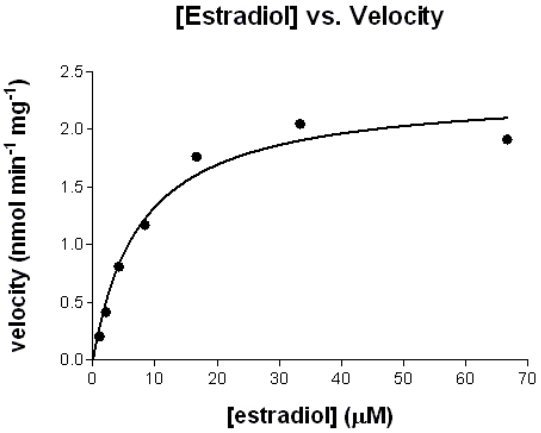

Biochemical Journal Immediate Publication. Published on 27 Oct 2006 as manuscript BJ20061319

Figure 3

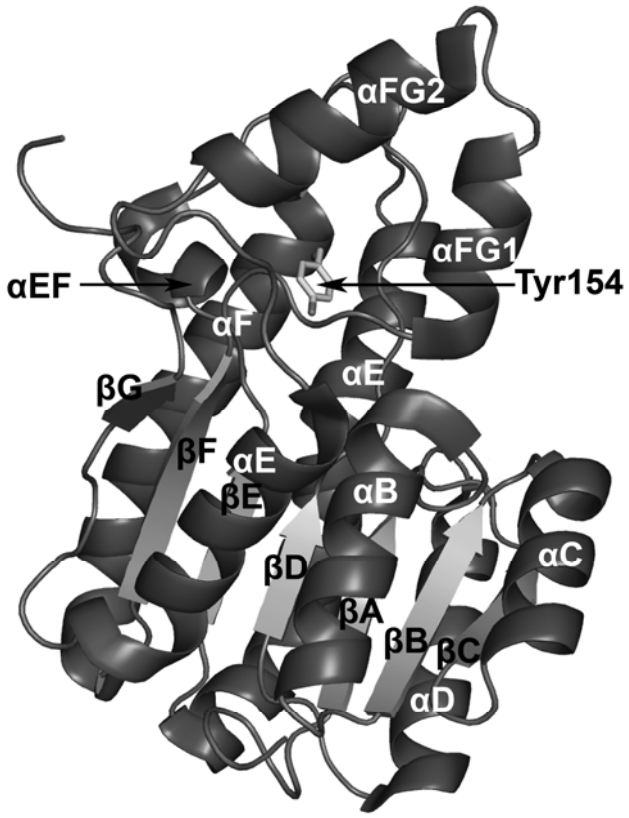

Biochemical Journal Immediate Publication. Published on 27 Oct 2006 as manuscript BJ20061319

Figure 4

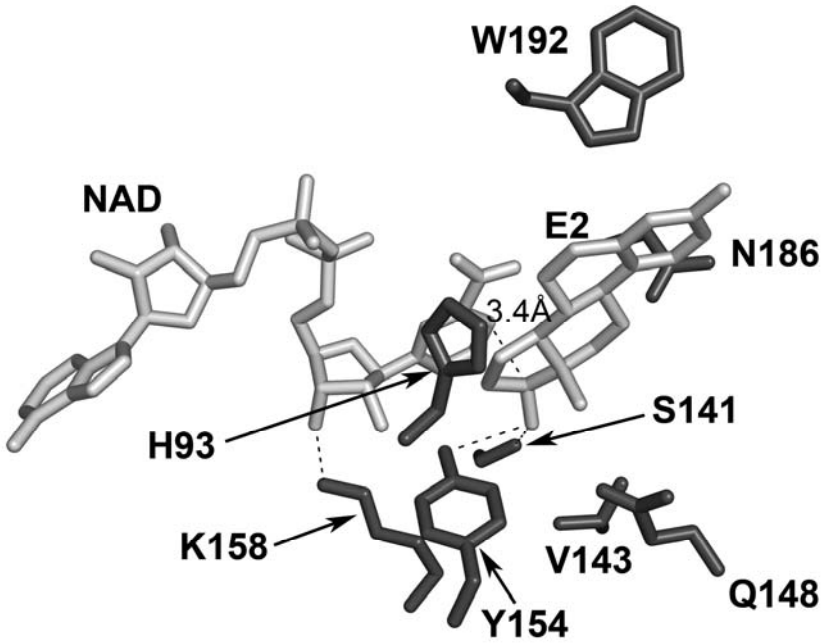

Biochemical Journal Immediate Publication. Published on 27 Oct 2006 as manuscript BJ20061319

Figure 5

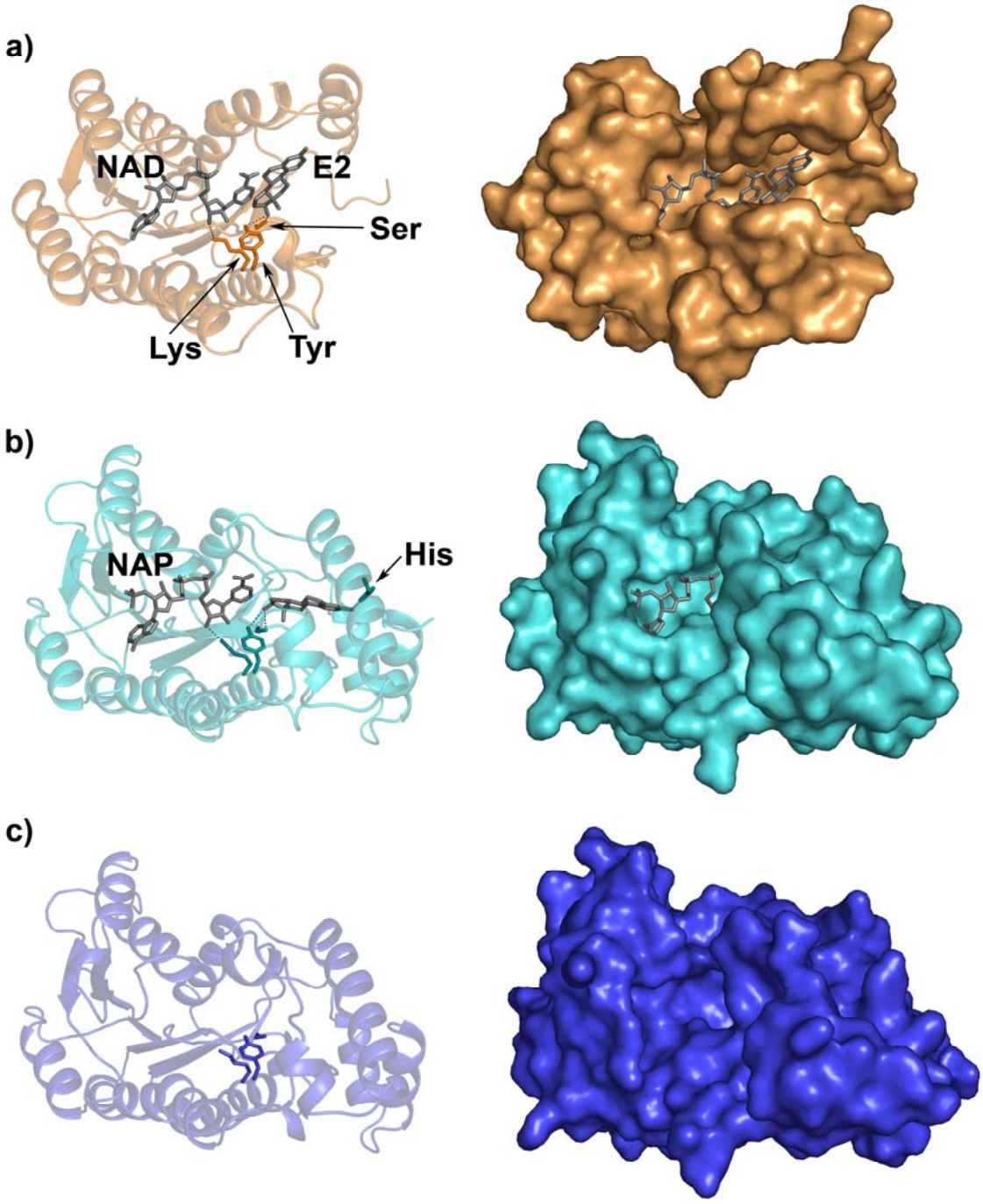

Biochemical Journal Immediate Publication. Published on 27 Oct 2006 as manuscript BJ20061319

Figure 6

Panel 1: DHRS10-GFP

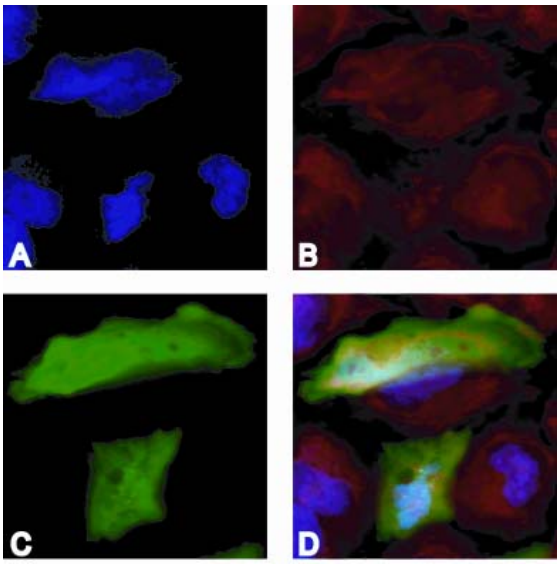

Panel 2: myc-DHRS10

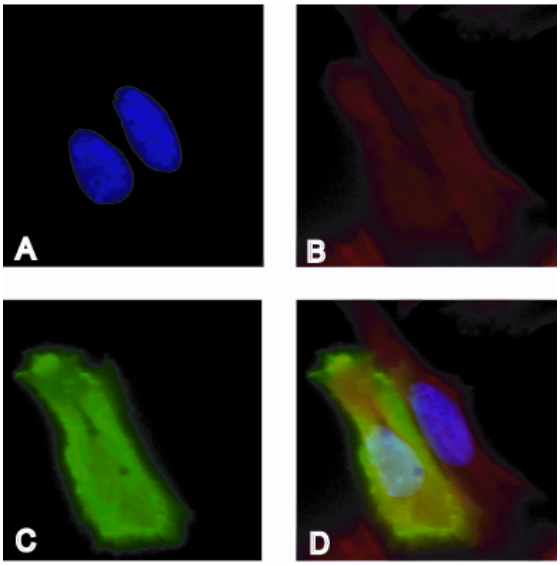

Biochemical Journal Immediate Publication. Published on 27 Oct 2006 as manuscript BJ20061319

Figure 7

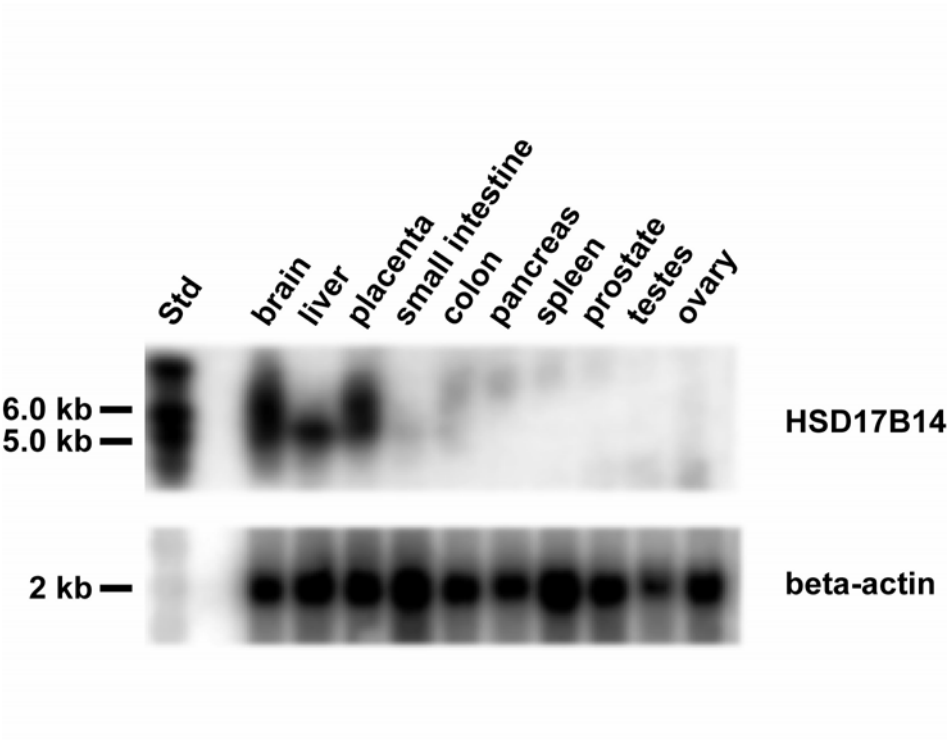

Legends to Figures

Figure 1: Multiple sequence alignment of selected human 17β-HSDs. Active site motifs (see text) are highlighted through boxing and marked by asterisks. Secondary structure elements as determined for DHRS10 are indicayed below the alignment as arrows (extended strands) and tubes (alpha helices).

Figure 2: a) *In vivo* kinetics for the formation of radioactively labeled estrone from estradiol over a period of time in Hek293T cells transfected with DHRS10. As a control, cells were also mock transformed with the pcDNA3 vector only. The net conversion is the percentage conversion carried out by DHRS10 transfected cells after subtracting the percentage conversion carried out by mock transfected cells at the same time point.
b) Typical separation of estradiol and estrone by HPLC. CPS - counts per second, rt - retention time, E2 - estradiol, E1 - estrone. Unlabeled peaks correspond to autoradiolytic products of substrate (estradiol) decay.
c) Michaelis-Menten Plot for the *in vitro* conversion of NAD^+ to NADH in the presence of estradiol.

Figure 3: The secondary structure of DHRS10. The side chain of the catalytic Tyr 154 is shown in stick representation. (All structural representations are drawn with the Program PyMOL.)

Figure 4: Detailed view of the active site of DHRS10. Modelled NAD and estradiol are shown in grey stick representation and side chains of residues belonging to DHRS10 are shown in dark grey stick representation. The distance measurement (3.4 Å) between C4 of nicotinamide and C17 of the steroid is shown in black dashed line and other polar contacts under 3.2Å are shown in unlabeled dashed lines.

Figure 5: Comparison of the DHRS10 structure with the structures of ternary complex and apoenzyme 17β-HSD1: The panels on the left show the various structures in ribbon representation set at 80% transparency and the panels on the right show the structures in the same orientation in surface representation.

a) The structure of DHRS10 apoenzyme (PDB code 1YDE) with modelled NAD and estradiol (E2) shown in grey stick representations. The catalytic residues Tyr 154, Lys 158 and Ser 141 are in orange stick representation.
b) The crystal structure of the 17β-HSD1 ternary complex containing NADP (NAP) and estradiol (E2) (PDB code 1FDT). The catalytic residues Tyr 155, Lys 159 and Ser 142 are shown in cyan stick representation.
c) The structure of the 17β-HSD1 (PDB code 1BHS) apoenzyme. The catalytic residues are shown in blue stick representation.

Figure 6: Cytosolic localization of human DHRS10. A. The top left insert of panel 1 shows nuclear counterstaining with the blue fluorescent dye Hoechst 33342, top right shows mitochondrial counterstaining with the orange fluorescent dye MitoTracker orange, bottom left shows green fluorescence due to expression of GFP tag at the C-terminus of DHRS10. The bottom right insert is an overlay of the previous three inserts. Panel 2 is arranged as above except that bottom left panel shows immunofluorescence due to the probing of the myc tag at the N-terminus of DHRS10 with a primary anti-myc 9B11 mouse monoclonal antibody and a secondary green fluorescent Alexa Fluor goat anti-mouse IgG antibody.
Panel 1: A = nuclear staining, B = mitochondrial staining, C = GFP, D = overlay
Panel 2: A = nuclear staining, B = phalloidin staining, C = myc tag detection with FITC labelled antibody, D = overlay.

Figure 7: Northern Blot analysis of DHRS10 in human tissues. mRNA from various human tissues was probed with a P^{32}-labelled DHRS10 probe. RNA molecular size standards are shown on the left hand side. Loading control hybridisation with a P^{32} labelled probe for beta-actin is also shown.